

# Influence of the Molecular Weight on the Inverse Temperature Transition of a Model Genetically Engineered Elastin-like pH-Responsive Polymer

Alessandra Girotti,<sup>†</sup> Javier Reguera,<sup>†</sup> Francisco Javier Arias,<sup>‡</sup> Matilde Alonso,<sup>§</sup> Ana María Testera,<sup>⊥</sup> and José Carlos Rodríguez-Cabello<sup>\*,†</sup>

Dpto. Física de la Materia Condensada, E.T.S.I.I., Universidad de Valladolid, Paseo del Cauce s/n, 47011 Valladolid, Spain; Dpto. Bioquímica, Biología Molecular y Fisiología, Facultad de Ciencias, Universidad de Valladolid, Dr. Mergelina s/n, 47005 Valladolid, Spain; Dpto. Química Analítica, E.U.P., Universidad de Valladolid, Francisco Mendizabal 1, 47014 Valladolid, Spain; and Dpto. Química Orgánica, E.T.S.I.I., Universidad de Valladolid, Paseo del Cauce s/n, 47011 Valladolid, Spain

Received October 24, 2003; Revised Manuscript Received February 24, 2004

**ABSTRACT:** The pH-responsive elastin-like polymers, [(PGVGV)<sub>2</sub>–(PGEV)]<sub>n</sub> with  $n = 5, 9, 15, 30, 45$ , were obtained using genetic engineering and microbial protein expression. These were intended to study the effects of the molecular weight (MW) on the properties of their inverse temperature transition (ITT) and its dependence on pH. As a result, the transition temperature decreased and the transition enthalpy increased as the molecular weight increased, especially for the lowest MWs. More strikingly, the apparent  $pK_a$  for the  $\gamma$ -carboxyl residue of the glutamic acid also depends on MW. The apparent  $pK_a$  is lower for lower MWs. In summary, the modification in the ITT caused by changes in MW is similar to the one caused by changes in the mean polarity of the polymer as described in the literature. A reduction in the molecular weight is equivalent to a decrease in the mean hydrophobicity of the polymer.

## Introduction

In the past years, the interest in protein-based polymers ("PBPs") is rapidly growing. This is especially true nowadays after the incorporation of recombinant DNA technologies, which have revolutionized the design and production of unique PBPs.<sup>1</sup> From the point of view of macromolecular science, the use of tailored DNA templates as the base of their bioproduction provides a tight, practically absolute, control of the sequence and polymer architecture, with the inexistence of randomness in amino acid stereochemistry, comonomer arrangement, and molecular weight (MW). In this manner, the obtaining of complex and monodisperse polymers with a desired sequence and molecular architecture is achievable in a quite natural way.<sup>2–4</sup> Additionally, the advantages of bioproduction include their environmental-friendly bioproduction and disposal.<sup>1,5</sup>

Among PBPs, elastin-like polymers (ELPs) are emerging as a new class of polymers with exceptional properties.<sup>6</sup> These include mechanical properties ranging from excellent elastomers to plastics, outstanding biocompatibility,<sup>7</sup> and acute smart behavior.<sup>6</sup> This last attribute is caused by the so-called "inverse temperature transition" (ITT). ITT has become the key issue in the development of new peptide-based polymers as molecular machines and materials. The understanding of the macroscopic properties of these materials in terms of the molecular processes taking place around the ITT has established the basis for their functional and rational design.<sup>8</sup>

All the functional elastin-like polymers exhibit phase transitional behavior associated with the ITT.<sup>6</sup> In aqueous solution and below a certain critical temperature ( $T_i$ ), the free polymer chains remain disordered, random coils in solution<sup>9</sup> that are fully hydrated, mainly by hydrophobic hydration.<sup>6,10</sup> On the contrary, above  $T_i$ , the chain hydrophobically folds and assembles to form a phase-separated state<sup>11</sup> in which the polymer chains adopt a dynamic, regular, nonrandom structure, called a  $\beta$ -spiral, involving one type II  $\beta$ -turn per pentamer, and stabilized by intraspinal interturn and interspiral hydrophobic contacts.<sup>6</sup> This is the product of the ITT. During the initial stages of polymer dehydration, hydrophobic association of  $\beta$ -spirals takes on fibrillar form that grows to a several hundred nanometer particle before settling into the visible phase-separated state.<sup>6,12</sup>

The design of smart polymers, responding to stimuli different than temperature changes, makes use of the " $\Delta T_i$  mechanism" and the "amplified  $\Delta T_i$  mechanism".<sup>6,13–15</sup> This is also the situation for the polymers studied in this work, in which the  $\gamma$ -carboxylic function of the glutamic acid suffers strong polarity changes between its protonated and deprotonated state as a consequence of changes in pH around its effective  $pK_a$ .

Taking advantage of the essentially monodisperse nature of these genetically engineered polymers, the influence of MW on the characteristics of the ITT displayed by this model polymer will be studied in this work.

The effect of MW on  $T_i$  has been previously addressed by Meyer and Chilkoti in a set of unfunctionalized (thermo-responsive) ELPs based on the sequence VPGXG ( $X = V, A, \text{ or } G$ ), taking advantage of the development of a new gene construction based on recursive directional ligation.<sup>16</sup> However, the use of carboxyl-functionalized polymers opens the possibility to extend the study of the MW influence to parameters such as  $pK_a$ , transi-

<sup>†</sup> Dpto. Física de la Materia Condensada.

<sup>‡</sup> Dpto. Bioquímica.

<sup>§</sup> Dpto. Química Analítica.

<sup>⊥</sup> Dpto. Química Orgánica.

\* To whom correspondence should be addressed: e-mail: cabello@eis.uva.es.

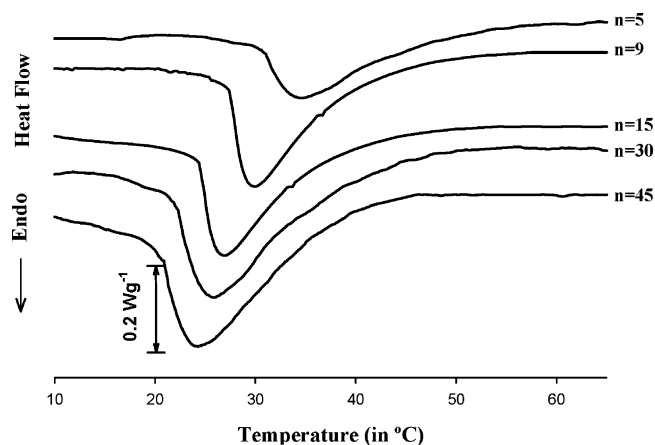


**Figure 1.** DSC thermograms of 50 mg mL<sup>-1</sup> phosphate buffered (0.1 M, pH 2.5) water solutions of the studied polymers. Their polymerization degree ( $n$ ) is shown on the right side of the plot. Heating rate 10 °C min<sup>-1</sup>.

tion enthalpy, and pH-dependent response. This is the objective pursued in this work.

### Experimental Section

**Materials.** *E. coli* strain BLR(DE3) and pET-25(+) were obtained from Novagen (Madison, WI). *Taq* DNA polymerase was purchased from Stratagene (La Jolla, CA); T4 DNA ligase and all restriction enzymes were obtained from New England Biolabs (Beverly, MA). Synthetic oligonucleotides were purchased from IBA GmbH (Goettingen, Germany).

**Synthetic Gene Construction.** Cloning and molecular biology techniques were performed using standard procedures,<sup>17,18</sup> and the sequence of all putative inserts was verified by automated DNA sequencing. A synthetic DNA duplex encoding the oligopeptide (VPGVG)<sub>2</sub>VPGE(VPGVG)<sub>2</sub> was generated by polymerase chain reaction (PCR) amplification using synthetic oligonucleotides. The gene cloning, concatenation and colony screening were performed as described in ref 19.

**Expression and Purification.** Selected genes were subcloned into a modified pET-25(+) expression vector and transformed into the *E. coli* strain BLR(DE3). Expression conditions and the purification protocol are described in refs 19 and 5, respectively. Production yields for the five polymers of general formula [(VPGVG)<sub>2</sub>VPGE(VPGVG)<sub>2</sub>]<sub>*n*</sub> selected for this work were 32 mg/L ( $n = 5$ ), 84 mg/L ( $n = 9$ ), 92 mg/L ( $n = 15$ ), 90 mg/L ( $n = 30$ ), and 47 mg/L ( $n = 45$ ). The final products were characterized by SDS-PAGE, MALDI-TOF mass spectrometry, NMR, and amino acid analysis. All the analysis confirms the correctness of the biosynthesis process in terms of sequence and MW.

**Differential Scanning Calorimetry (DSC).** DSC experiments were performed on a Mettler Toledo 822<sup>e</sup> with liquid nitrogen cooler. Calibration of both temperature and enthalpy was made with a standard sample of indium. For DSC analysis, phosphate buffered (0.1 M) water solutions of the polymers were prepared at different pHs and concentrations (see text). In a typical DSC run, 25  $\mu$ L of the solution was placed inside a standard 40  $\mu$ L aluminum pan hermetically sealed. The same volume of water was placed in the reference pan. All DSC samples were pretreated 15 min at 5 °C inside the sample chamber just before the beginning of the experiment.

### Results and Discussion

Figure 1 shows DSC analysis of the five polymers in phosphate buffer (pH = 2.5). This pH is considered to be low enough to yield a complete protonation of all  $\gamma$ -carboxyl residues in the polymers. The thermograms showed the typical endotherm associated with the ITT.

According to previous work, these endotherms are the net result of two concurrent events with separate thermal contribution: an endothermic component due to loss of hydrophobic hydration and an oppositely signed exothermic component due to the physical association of chains, the endothermic component being predominant.<sup>20</sup> Some qualitative differences between the five MWs are apparent from this figure. In general, the peak temperature of each endotherm, which can be identified with the transition temperature at this pH ( $T_{i0}$ ), tends to be higher for lower MW. On the contrary, the transition enthalpy at this same pH ( $\Delta H_0$ ) tends to increase with the increasing MW.

A polymer concentration of 50 mg mL<sup>-1</sup> was initially adopted in this work as working concentration to perform the DSC analysis. However, the first question that arises on the suitability of the used conditions to follow the dependence of the transition parameters vs MW is the potential influence of the polymer concentration on  $T_{i0}$  and  $\Delta H_0$ . Previous works have shown that, in particular,  $T_i$  can be strongly affected by polymer concentration in two different ways. At low concentrations,  $T_i$  values tend to increase for decreasing concentrations.<sup>6</sup> This has been interpreted as the effect of an interchain cooperativity taking place during the chain folding, so in dilute conditions this effect cannot take place appropriately.<sup>6</sup> However, there is a concentration limit where this effect disappears, and further increases in the polymer concentration do not cause  $T_i$  changes. For a chemically synthesized poly(VPGVG), this concentration limit was reached at about 20–40 mg mL<sup>-1</sup> (see ref 6).

Additionally, there is a second circumstance by which  $T_i$  further changes with polymer concentration. This happens when the concentration of the unfolded state is too high for its complete hydration. Under this situation, the increase in concentration causes again an increase in  $T_i$ , which, in this turn, is accompanied by a parallel decrease in  $\Delta H$ . Again, for a chemically synthesized poly(VPGVG), this water deficiency limit<sup>10</sup> has been estimated around 125 mg mL<sup>-1</sup>. Although the working concentration adopted here, 50 mg mL<sup>-1</sup>, is within the limits found for poly(VPGVG), the different composition of the polymer used in this work makes necessary to test whether this concentration is within the adequate limits. Therefore, the influence of polymer concentration on  $T_i$  and  $\Delta H$  has been studied for all the bioproducted polymers used in this work at five concentrations ranging between 20 and 100 mg mL<sup>-1</sup>. Figure 2 shows example results for the polymer with  $n = 15$ . It is evident from this figure that  $T_i$  does not show significant changes within this concentration range. Peak integral of the thermograms also indicates that  $\Delta H$  did not differ for the different concentrations used. This same result has been also found for the rest of MWs (result not shown). Therefore, the concentration of 50 mg mL<sup>-1</sup> adopted in this work can be considered within the safe concentration range.

A second source of artifacts that could cause misinterpretation of the experimental data comes from the dynamical nature of the DSC experiments. Although  $\Delta H$  values are not affected by the dynamical conditions of the DSC experiment, peak temperatures and accordingly  $T_i$  values are usually affected by thermal lags.<sup>21</sup> In addition, although not likely, some differences in  $C_p$  values could take place among the different samples.

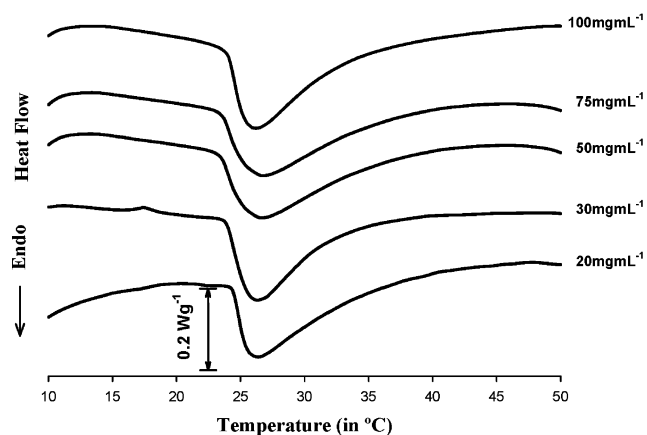


**Figure 2.** DSC thermograms of phosphate buffered (0.1 M, pH 2.5) water solutions of [(VPGVG)<sub>2</sub>VPGE(VPGVG)<sub>2</sub>]<sub>15</sub>. Polymer concentration is shown on the right side of the plot. Heating rate 10 °C min<sup>-1</sup>.

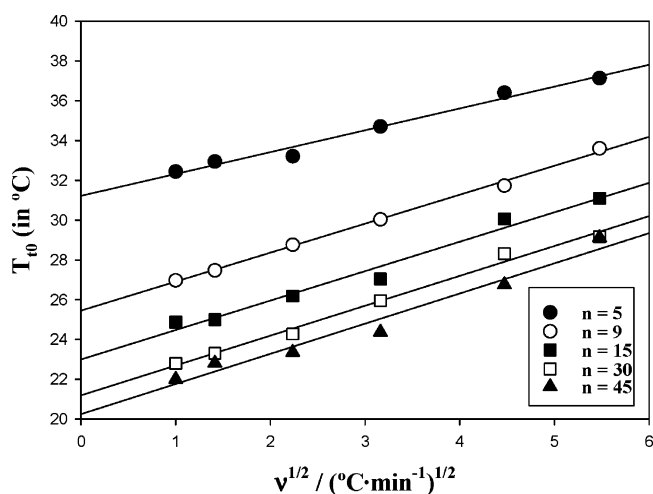


**Figure 3.** Dependence of  $T_0$  on the square root of the heating rate for the studied polymers. The corresponding polymerization degree ( $n$ ) is indicated in the plot. The lines represent the least-squares linear regressions of the data for each  $n$ .

That would give rise to different thermal lags among the samples so the observed differences in  $T_i$  among the different MWs could be, at least partially, caused by this effect. To test the impact of thermal lags in the  $T_0$  data, we have estimated the so-called “true  $T_0$ ” ( $T_{0}^{\text{true}}$ ) for the five MWs studied. According to literature, this temperature must be understood as the true physical point of the transition.<sup>21</sup> Adequate values of  $T_{0}^{\text{true}}$  can be obtained by extrapolation of the linear sections of the resulting plot of  $T_0$  vs the square root of the heating rate ( $\nu^{1/2}$ ) to  $\nu = 0$  (see ref 21). The results of this analysis are given in Figure 3, and a plot of  $T_{0}^{\text{true}}$  vs MW can be seen in Figure 4. As suspected from the qualitative analysis of the DSC results, the dependence of  $T_0$  on the polymer MW was not an artifact. There is a strong dependence that scores a difference of about 10 deg between the lowest ( $n = 5$ ) and highest molecular weight ( $n = 45$ ) tested in this work,  $T_0$  being lower for higher MWs. This dependence is not linear. The strongest variations in  $T_0$  were found in the lowest MWs. These results are in good agreement with those shown by unfuntionalized genetically engineered ELPs<sup>16</sup> and by previous ones obtained on MW fractions of chemically synthesized poly(VPGVG).<sup>6</sup> In all cases the strongest dependence was found for the lowest MWs with an asymptotic behavior for high MWs. The differences

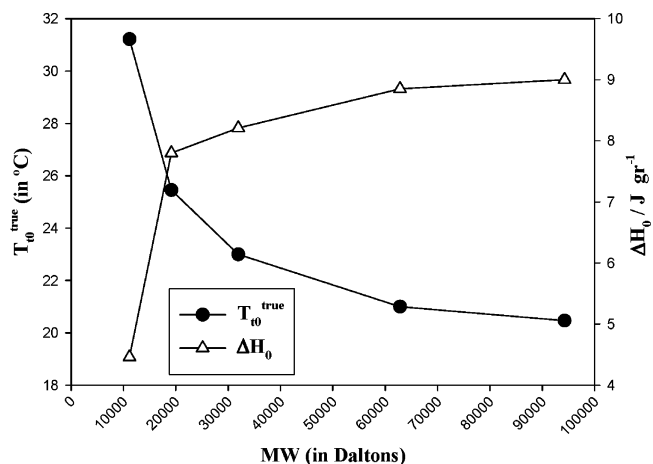


**Figure 4.** Dependence of  $T_{0}^{\text{true}}$  and  $\Delta H_0$  on the molecular weight.

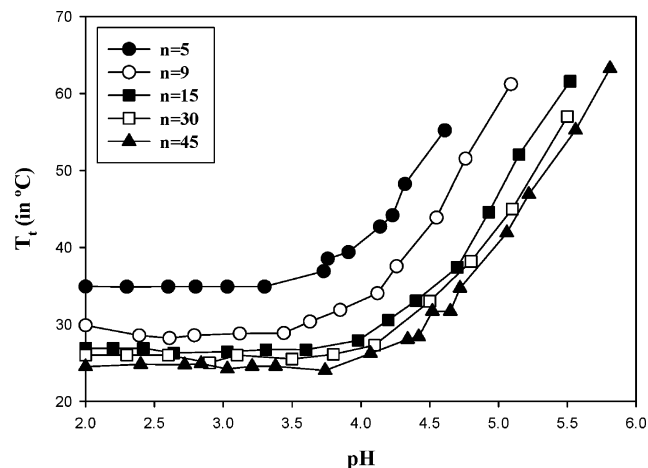


**Figure 5.** Dependence of  $T_i$  on the pH for the studied polymers (as indicated in the plot).

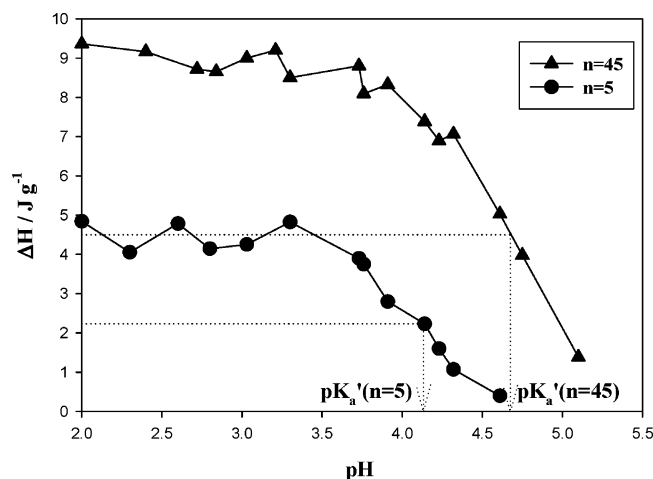
between those results and ours can be easily explained in terms of, first, the higher concentration buffer solution used in our work, since that condition was needed to achieve a enough buffer capacity at the relatively high polymer concentration necessary to obtain reliable DSC measurements. Other factors that can be origin of some minor disagreements come from the different composition of the polymers and, in the particular case of the chemically synthesized poly(VPGVG), to the asymmetric influence of the low MW tail and the differences in the MW dispersion within the different MW fractions used. Additionally, in some of these previously published data, the use of polymer concentrations below the low limit of the safe concentration range is also a probable source of discrepancies.

Figure 4 also shows the dependence of  $\Delta H_0$  on MW (pH = 2.5). As it happened with  $T_0$ , there is a clear dependence of this parameter on MW;  $\Delta H_0$  increases in a nonlinear manner as MW increases. The highest variations were found again for the lowest MWs.

It is of interest the influence of the pH on the ITT ( $T_i$  and  $\Delta H$ ) for this set of polymers. To study this, DSC analysis of phosphate buffered solutions has been carried out in a pH range from 2.0 to 5.5–6.0. The results for  $T_i$  as a function of pH are plotted in Figure 5.

The five polymers showed a similar trend. Up to a given pH,  $T_i$  values remain practically constant. Above this particular pH,  $T_i$  rapidly increases. A parallel inverted behavior was found for  $\Delta H$ ; the plot  $\Delta H$  vs pH





**Figure 6.** Dependence of  $\Delta H$  on the pH for the polymers with  $N = 5$  and  $45$  (as indicated in the plot). Dotted lines illustrate the procedure to estimate the apparent  $pK_a$  values ( $pK_a'$ ) for the  $\gamma$ -carboxyl group of the glutamic acid (see text).

can be seen in Figure 6 for the polymers with extreme MWs:  $n = 5$  and  $45$ . (The other MWs have not been plotted for clarity purposes). Again,  $\Delta H$  remains rather constant below the characteristic pH. However, at this given pH the enthalpy rapidly drops to zero. This behavior is the expected according to the literature<sup>6</sup> and can be easily explained. As a result of the increase in the pH, the  $\gamma$ -carboxyl group of the glutamic acid starts to become deprotonated. This deprotonation yields an increase in the mean polarity of the polymer which causes a  $T_i$  shift to higher temperatures and a drop in  $\Delta H$ , since this parameter depends primarily on the amount of hydrophobic hydration around the polymer, and this hydration mode is not possible in the vicinities of the charged carboxylate.<sup>6</sup> Thus, the pH pointing the onset of the increase in  $T_i$  and the decrease in  $\Delta H$  is related with the onset of the  $\gamma$ -carboxyl deprotonation. As can be seen in Figure 6, this pH is different for the different polymers.

Strikingly, this fact would imply that the equilibrium constant for the protonation–deprotonation of the  $\gamma$ -carboxyl group would depend on the MW. The apparent  $pK_a$  ( $pK_a'$ ) of the  $\gamma$ -carboxyl group has been estimated as the pH yielding a 50% drop in  $\Delta H$ , which, according to the molecular interpretation of  $\Delta H$ , can be roughly considered as the 50% deprotonated state of the free carboxyls. The dependence of  $pK_a'$  on MW can be seen in Figure 7. Again, the lowest MWs showed the strongest  $pK_a$  shifts to lower values, ranging from 4.13 for  $n = 5$  to 4.68 for  $n = 45$ .

This is not the first reported case where a  $pK_a$  value of a free carboxyl moiety is shifted as a consequence of changes in the intrinsic characteristic of the elastin-like polymer where this carboxyl is present. In ref 22, the effect of the increase in the mean hydrophobicity for a sequence of polymers with formulas poly[0.8(PGVGV), 0.2(PGEGV)], poly[0.8(PGVGI), 0.2(PGEGI)] (I stands for isoleucine), and poly[0.75(PGFGV), 0.25(PGEGV)] (F stands for phenylalanine) caused 1.7 units  $pK_a$  positive shift. In a later work from the same authors, by appropriate nanometric design of the polymer compositions, hydrophobic-induced  $pK_a$  shifts for aspartic acid as high as 6.2 units have been reported.<sup>23</sup> Upon comparison of the  $pK_a$  shifts found in this work as a consequence of changes in the MW and those found as consequence of changes in the mean polarity of the

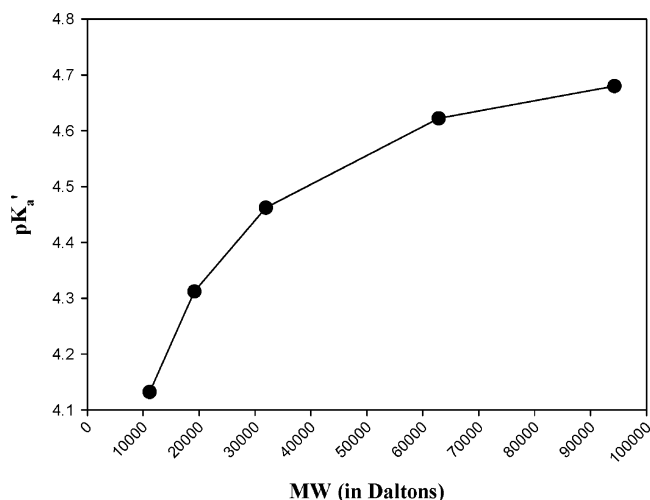


**Figure 7.** Dependence of  $pK_a'$  for the  $\gamma$ -carboxyl group of the glutamic acid on the molecular weight.

polymer, again a clear similarity between MW and the mean hydrophobicity is found. The  $pK_a$  shift observed as MW increases is equivalent to that caused by an increase in the mean hydrophobicity, in a similar way to that previously found for  $T_{i0}$  and  $\Delta H_0$ .

### Concluding Remarks

In summary, from the study of this set of model elastin-like polymers one can conclude that MW has an evident influence in the behavior and ITT parameters of this kind of smart polymers. The decrease in MW causes an increase in  $T_t$ , a decrease in  $\Delta H$ , and a  $pK_a$  shift to lower values. All these effects have been already reported for other elastin-like polymers as being caused by a reduction of the mean hydrophobicity of the polymer by selected substitution of the amino acids in the polymer chain. Therefore, there is certain equivalence between polymer length and polymer hydrophobicity. This equivalence could be partially explained by the influence of the polar chain-end groups, this influence being higher for lower molecular weights. Thus, the mean hydrophobicity would be lower for lower MWs. However, the exclusive effect of the end-chain polarity seems not to be enough to account for the strong influence reported in this work. We believe that a large part of the effect of MW on the ITT is caused by the inter- and intrachain cooperativity of the hydrophobic self-assembly taking place during the ITT.<sup>9</sup> In this sense, it is reasonable to think that short chains do not show an efficient cooperation so their self-assembly is hindered, just like the presence of polar moieties in longer polymer chains hinders the characteristic hydrophobic folding and self-assembly during the ITT.

**Acknowledgment.** This work was supported by the “Junta de Castilla y León” (Projects VA30/00B and VA002/02) and by the MCYT (Projects MAT2000-1764-C02-02 and MAT2001-1853-C02-01). J. Reguera was supported by a grant from the “Junta de Castilla y León” (program FPI). The authors want to acknowledge the inestimable help of Prof. T. Girbés.

### References and Notes

- (1) Ferrari, F. A.; Cappello, J. In *Protein-Based Materials*; McGrath, K., Kaplan, D., Eds.; Birkhauser: Boston, MA, 1997; p 37.

- (2) Panitch, A.; Yamaoka, T.; Fournier, M. J.; Mason, T. L.; Tirrell, D. A. *Macromolecules* **1999**, *32*, 1701–1703.
- (3) Cappello, J.; Crissman, J. W.; Crissman, M.; Ferrari, F. A.; Textor, G.; Wallis, O.; Whitley, J. R.; Zhou, X.; Burman, D.; Aukerman, L.; Stedronsky, E. R. *J. Controlled Release* **1998**, *53*, 105–117.
- (4) Urry, D. W. In *Biomaterials Handbook—Advanced Applications of Basic Sciences and Bioengineering*; Wise, D. L., Hasirci, V., Yaszemski, M. J., Altobelli, D. E., Lewandrowski, K. U., Trantolo, D. J., Eds.; Marcel Dekker: New York, 2003.
- (5) McPherson, D. T.; Xu, J.; Urry, D. W. *Protein Expression Purif.* **1996**, *7*, 51–57.
- (6) Urry, D. W. *Angew. Chem., Int. Ed. Engl.* **1993**, *32*, 819–841.
- (7) Urry, D. W.; Parker, T. M.; Reid, M. C.; Gowda, D. C. *J. Bioact. Compat. Pol.* **1991**, *6*, 263–283.
- (8) Urry, D. W. *J. Phys. Chem. B* **1997**, *101*, 11007–11028.
- (9) San Biagio, P. L.; Madonia, F.; Trapane, T. L.; Urry, D. W. *Chem. Phys. Lett.* **1988**, *145*, 571–574.
- (10) Rodríguez-Cabello, J. C.; Alonso, M.; Pérez, T.; Herguedas, M. M. *Biopolymers* **2000**, *54*, 282–288.
- (11) Urry, D. W.; Trapane, T. L.; Prasad, K. U. *Biopolymers* **1985**, *24*, 2345–2356.
- (12) Manno, M.; Emanuele, A.; Martorana, V.; San Biagio, P. L.; Bulone, D.; Palma-Vittorelli, M. B.; McPherson, D. T.; Xu, J.; Parker, T. M.; Urry, D. W. *Biopolymers* **2001**, *59*, 51–64.
- (13) Rodríguez-Cabello, J. C.; Alonso, M.; Guiscardo, L.; Reboto, V.; Girotti, A. *Adv. Mater.* **2002**, *14*, 1151–1154.
- (14) Alonso, M.; Reboto, V.; Guiscardo, L.; San Martín, A.; Rodríguez-Cabello, J. C. *Macromolecules* **2000**, *33*, 9480–9482.
- (15) Alonso, M.; Reboto, V.; Guiscardo, L.; Maté, V.; Rodríguez-Cabello, J. C. *Macromolecules* **2001**, *34*, 8072–8077.
- (16) Meyer, D. E.; Chilkoti, A. *Biomacromolecules* **2002**, *3*, 357–367.
- (17) Sambrook, J.; Fritsch, E. F.; Maniatis, T. *Molecular Cloning: A Laboratory Manual*; Cold Spring Harbor Laboratory Press: Cold Spring Harbor, NY, 1992.
- (18) McMillan, R. A.; Lee, T. A. T.; Conticello, V. P. *Macromolecules* **1999**, *32*, 3643–3648.
- (19) Girotti, A.; Arias, F. J.; Reguera, J.; Alonso, M.; Testera, A. M.; Rodríguez-Cabello, J. C. *J. Mater. Sci.-Mater. M* **2004**, *15*, 477–482.
- (20) Rodríguez-Cabello, J. C.; Reguera, J.; Alonso, M.; Parker, T. M.; McPherson, D. T.; Urry, D. W. *Chem. Phys. Lett.* **2004**, *388*, 127–131.
- (21) Bershtein, V. A.; Egorov, V. M. *Differential Scanning Calorimetry of Polymers. Physics, Chemistry, Analysis, Technology*; Ellis Horwood: London, 1994.
- (22) Urry, D. W.; Peng, S. Q.; Parker, T. M. *Biopolymers* **1992**, *32*, 373–379.
- (23) Urry, D. W.; Gowda, D. C.; Peng, S.; Parker, T. M.; Jing, N.; Harris, R. D. *Biopolymers* **1994**, *34*, 889–896.

MA035603K